PHYSICAL REVIEW E **73**, 055202(R) (2006)

Universal behavior in populations composed of excitable and self-oscillatory elements

Diego Pazó[1,*] and Ernest Montbrió[2,3,4]

[1]*Max-Planck-Institut für Physik komplexer Systeme, Nöthnitzer Straße 38, 01187 Dresden, Germany*

[2]*Departament de Física, Universitat de les Illes Balears, E-07122 Palma de Mallorca, Spain*

[3]*Institut Mediterrani d'Estudis Avançats, IMEDEA (CSIC-UIB), E-07122 Palma de Mallorca, Spain*

[4]*Computational Neuroscience, Technology Dept., Universitat Pompeu Fabra, 08003 Barcelona, Spain*

(Received 1 September 2005; published 31 May 2006)

We study the robustness of self-sustained oscillatory activity in a globally coupled ensemble of excitable and oscillatory units. The critical balance to achieve collective self-sustained oscillations is analytically established. We also report a universal scaling function for the ensemble's mean frequency. Our results extend the framework of the "aging transition" [Phys. Rev. Lett. **93**, 104101 (2004)] including a broad class of dynamical systems potentially relevant in biology.

DOI: 10.1103/PhysRevE.73.055202 PACS number(s): 05.45.Xt, 87.10.+e

Large networks of interacting dissipative systems are appropriately modeled in terms of coupled nonlinear differential equations, which successfully reproduce a huge variety of the dynamical patterns found in nature. In many cases, the individual systems present time-periodic behavior and may achieve a certain degree of global synchronization despite the unavoidable differences among them [1,2]. This subject has attracted a great deal of both theoretical and experimental interest during the past decades [3].

However, the robustness of the macroscopic synchronized oscillations in a mixed population of self-oscillatory and non-self-oscillatory elements has only been addressed very recently by Daido and Nakanishi [4]. Interestingly, they report a general scenario, called "aging transition," characterized by a universal (i.e., independent of the oscillator type) scaling function. In [4] the aging transition was found in populations of oscillators in which some of them lose their self-oscillatory activity (by deterioration or "aging") through an inverse Hopf bifurcation.

In this Rapid Communication we present an extension of the aging transition taking place in a new class of systems in which the oscillatory behavior is lost in a saddle-node (SN) bifurcation. Such systems are of particular relevance since their resulting dynamics is excitable and thus of interest in many areas of physics, chemistry, and biology [1,5–7].

For instance, a remarkable example of macroscopic synchronization is found among the pacemaker cells in the sinoatrial node which initiate the heartbeat. When a certain ratio of cells are damaged by disease, the lack of an adequate synchronized state requires the implantation of an electronic pacemaker. Nevertheless, new techniques aiming to create biological pacemakers have been recently proposed as a very promising alternative to electronic ones [8]. One of them consists in the creation of an aggregate of biological pacemaker cells in some region(s) of the ventricle, converting excitable heart cells into pacemaker cells by gene transfer [9], in an "inverse-aging" transition. This is feasible since the heart's pacemaker and excitable cells are very similar (they are both identical pacemaker cells in the early embryonic heart, and differentiate as the development progresses). In this context, the robustness of the aggregate's self-oscillating activity in a mixed population of self-oscillatory (converted) and excitable (unaltered) elements seems to be particularly relevant.

In our study, we have considered systems that cease their oscillatory behavior through a SN bifurcation on invariant circle (SNIC) [7], also called SN homoclinic bifurcation [10] (see Fig. 1). This is the simplest possible scenario linking excitable and oscillatory dynamics, and there is only one attractor at each parameter value. The excitable regime (at one side of the bifurcation) is very well known in theoretical neuroscience, where it is referred to as class I excitability [11].

Additionally, we make the following assumptions.

(i) The population (of size N) is divided into two groups, consisting of pN $[1/N \leqslant p \leqslant (N-1)/N]$ identical excitable units (S_E), and of $(1-p)N$ identical active units (S_A). The elements in the population are ordered according to an index j, such that $S_A \equiv j \in \{1,\ldots,(1-p)N\}$ and $S_E \equiv j \in \{(1-p)N+1,\ldots,N\}$.

(ii) A linear all-to-all coupling is assumed, for the state variable $\mathbf{x}_j$ of each unit:

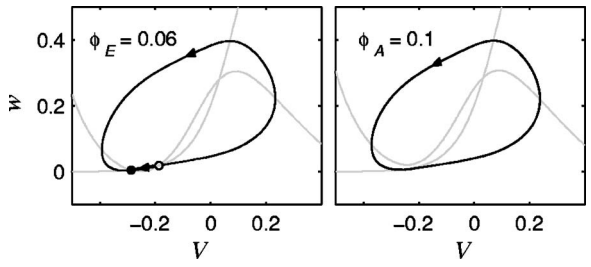

FIG. 1. Morris-Lecar equations (2) in the excitable (left panel) and in the oscillatory (right panel) regimes. Both dynamical states are linked through a saddle-node bifurcation on invariant circle (SNIC) at $\phi^* \simeq 0.076$ [see Eq. (2a)]. The nullclines $\dot{V}=0$ and $\dot{w}=0$ are depicted with gray lines.

*Present address: Instituto de Física de Cantabria (CSIC-UC), E-39005 Santander, Spain.

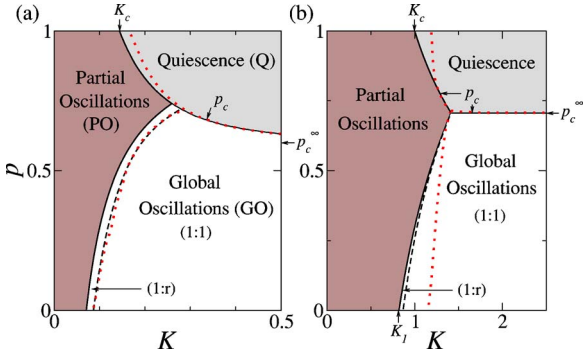

FIG. 2. (Color online) (K,p) phase diagram for a mixed population of oscillatory and excitable elements: (a) Morris-Lecar (2) with $\phi_A=0.1$ and $\phi_E=0.06$; (b) phase model (3) with $b_A=0$ (oscillatory) and $b_E=\sqrt{2}$ (excitable). Inside the region of global oscillations (GO) the black dashed line separates 1:1 (right) from other $1:r$, $0<r<1$ (left) frequency ratios, within the region GO. The (red, online) dotted curves are the deformation of the solid lines when heterogeneity in each subpopulation is considered (see text): γ=(a) 0.01 and (b) 0.6.

$$\dot{\mathbf{x}}_j = \mathbf{F}_j(\mathbf{x}_j) + \frac{K}{N}\sum_{k=1}^{N}(\mathbf{x}_k - \mathbf{x}_j), \tag{1}$$

where $\mathbf{F}_j=\mathbf{F}_A$ for $j\in S_A$ and $\mathbf{F}_j=\mathbf{F}_E$ for $j\in S_E$. In general, the coupling term in (1) could simply enter through a single variable of $\mathbf{x}_j$ (e.g., the membrane potential, in a cell model). This has in many cases the same synchronizing effect (but see [12]).

First we introduce our findings using an ensemble of globally coupled Morris-Lecar (ML) units [13]. The ML equations were obtained from the study of the electrical activity of the barnacle muscle fiber, and later they were popularized as a reduced model of excitability [11]. We have used the adimensionalized version proposed in [14], with the coupling term (proportional to K) entering through the voltage variable. The system is

$$C\dot{V}_j = g_L(-V_L - V_j) + g_{Ca}m_\infty(V_j)(V_{Ca} - V_j) - g_K w_j(V_K + V_j) + \phi_j(0.2 - V_j) + \frac{K}{N}\sum_{i=1}^{N}(V_i - V_j), \tag{2a}$$

$$\dot{w}_j = \lambda(V_j)[w_\infty(V_j) - w_j], \tag{2b}$$

where $m_\infty(V_j)=0.5\{1+\tanh[(V_j-v_1)/v_2]\}$, $w_\infty(V_j)=0.5\{1+\tanh[(V_j-v_3)/v_4]\}$, and $\lambda(V_j)=\lambda_0\{1+\cosh[(V_j-v_3)/v_4]\}$. Several constants [19] were taken from [14] with the external current set equal to zero. The term $\phi_j(0.2-V_j)$ in Eq. (2a) controls the dynamics of an isolated element [20]. In our model ϕ_j takes only two possible values ϕ_A and ϕ_E. For $\phi_A>\phi^*\simeq 0.076$ the dynamics of an isolated cell is self-oscillatory, whereas for $\phi_E<\phi^*$ it is excitable. Both behaviors are linked by a SNIC at ϕ^* (Fig. 1).

The system (2) is described in terms of two control parameters, the ratio p of excitable units, and the coupling strength K. Figure 2(a) shows the (K,p) phase diagram with the dynamical regimes found in the ensemble of ML units. For small coupling K, each element in the population essentially maintains its intrinsic dynamics. Such a state is labeled as partial oscillations (PO) because the collective state is not entirely oscillatory (the excitable elements are not able to oscillate, they only exhibit small amplitude "pulsations"). For large values of the coupling strength K, all the elements in the ensemble exhibit the same behavior, but depending on the ratio p they are all at rest [quiescence Q] or all oscillating [global oscillations (GO)]. The region GO contains a thin stripe-shaped subregion, where all the units are oscillating, but with frequency ratios different from 1:1.

The structure of the parameter space in Fig. 2(a) is reproduced for other oscillator types like the one proposed by Eguia *et al.* [15] and a phase model close to a SNIC (so-called "active rotator" [16]). The equations for the globally coupled phase model are

$$\dot{\theta}_j = 1 - b_j \sin\theta_j + \frac{K}{N}\sum_{l=1}^{N}\sin(\theta_l - \theta_j), \tag{3}$$

where the parameter b_j characterizes the nonuniformity of the phase rotation. Figure 2(b) shows that the simple phase model (3) qualitatively behaves as the ensemble of ML oscillators [Fig. 2(a)]. The only significant difference is the shape of the region inside GO with different rotation numbers in each subpopulation: wedge-shaped for the phase model and stripe-shaped for "complete" models. For phase models (other implementations were tested), leaving the Q region implies generically a transition to GO with 1:1 frequency ratio, or to PO (1:0). For coupled oscillators, the transition from the quiescent state to oscillations with other frequency ratios $(1:r)$ is of codimension one. From our simulations with the ML equations we have indications that in this transition the structure of phase space is a Cherry flow (see, e.g., [17]), although this seems difficult to prove.

In order to check the robustness of the diagrams in Fig. 2 we performed numerical simulations (N=1000) considering a certain degree of heterogeneity in each subpopulation (see red dotted lines in Fig. 2). This has been carried out distributing the systems' parameters uniformly around $\phi_{A,E}$ (ML) and $b_{A,E}$ (phase model) with a finite width γ. Heterogeneity shrinks the region Q, since there is need of more coupling strength to counterbalance the major diversity in the population. As a last remark, we just notice that the dynamics in the PO and GO regions become more complex (some regimes cannot be labeled by just one frequency ratio).

The rest of this Communication is devoted to the analysis of Fig. 2 in the absence of heterogeneity (i.e., $\gamma=0$). We will mainly stress those results whose validity is independent irrespective of the particular dynamical system considered. One empirical fact that simplifies the analysis is that in the whole K-p plane all the identical elements are at the same state: $\mathbf{x}_{j\in S_A}=\mathbf{x}_A, \mathbf{x}_{j\in S_E}=\mathbf{x}_E$. Thus, it is possible to study the dynamics of the population in terms of two asymmetrically coupled elements:

$$\dot{\mathbf{x}}_A = \mathbf{F}_A(\mathbf{x}_A) + Kp(\mathbf{x}_E - \mathbf{x}_A), \tag{4a}$$

$$\dot{\mathbf{x}}_E = \mathbf{F}_E(\mathbf{x}_E) + K(1-p)(\mathbf{x}_A - \mathbf{x}_E), \tag{4b}$$

with $\mathbf{x}=(V,w)$ for the ML cells, and $\mathbf{x}=\theta$ for the phase model. This simplification allows us to study the $N\to\infty$ limit and to adjust p continuously. In fact, reduction (4) was used to efficiently compute Fig. 2. And, in particular, for the phase model (3), the bifurcation lines limiting Q can be easily calculated analytically for $b_A=0$: $p_c=1/K$ and $p_c=1/b_E$, with a degenerate point at $(K,p)=(b_E,b_E^{-1})$. Other lines must be computed numerically [21].

An important feature of the phase diagrams in Fig. 2 is the asymptotic value of the bifurcation line limiting Q: $p_c^\infty \equiv p_c(K\to\infty)$. Remarkably, p_c^∞ can be analytically estimated in a simple way. The calculation is based on the fact that close to p_c the dynamics evolves for a long time inside a (slow) region where the SN bifurcation takes place. Therefore, resorting to the normal form of a SN bifurcation, we obtain (after rescaling space and time)

$$\dot{z}_A = a\epsilon_A - z_A^2 + Kp(z_E - z_A), \tag{5a}$$

$$\dot{z}_E = a\epsilon_E - z_E^2 + K(1-p)(z_A - z_E), \tag{5b}$$

with $\epsilon_A<0$ and $\epsilon_E>0$ according to the oscillatory (no fixed point) and the excitable (one stable and one saddle fixed point) regimes at both sides of the SN bifurcation (at $\epsilon=0$). In the limit $K\to\infty$, the quadratic terms can be neglected at the bifurcation point. From the nullclines of Eq. (5) $[z_E=z_A-(a\epsilon_A-z_A^2)/Kp$ and $z_A=z_E-(a\epsilon_E-z_E^2)/K(1-p)]$ we obtain

$$p_c^\infty = \frac{\epsilon_A}{\epsilon_A - \epsilon_E}. \tag{6}$$

This is one of the main results of the present work. Equation (6) gives the critical proportion of excitable and oscillatory elements in order for the whole population to become self-oscillatory. Only three parameters are needed: the value of the control parameter at the SN bifurcation and the distances, ϵ_A and ϵ_E, of the oscillatory and excitable elements to the bifurcation point. Specifically, for the ML model we have $\epsilon_{A,E}\simeq(\phi^*-\phi_{A,E})$, that according to (6) yields $p_c^\infty\simeq 0.60$, in good agreement with the numerical results (see also Fig. 3) [22]. Remarkably we find that Eq. (6) holds also for an ensemble of dynamical systems at both sides of a *Hopf* bifurcation [we skip here the proof, but cf. Eq. (4) in [4] for a particular case].

Our next results concern the behavior of the mean ensemble's frequency, which is a natural measure for the global oscillatory activity. The ensemble's average of the individual frequencies is

$$\Omega = \frac{1}{N}\sum_{j=1}^{N}\Omega_j, \tag{7}$$

where Ω_j represents the mean frequency of the jth element. Obviously, under the assumption in Eq. (4), $\Omega=(1-p)\Omega_A+p\Omega_E$ (with $\Omega_A=\Omega_{j\in S_A}$, $\Omega_E=\Omega_{j\in S_E}$). Figure 3 shows the average frequency (7)—normalized by the frequency at $p=0$: $\tilde{\Omega}(p)\equiv\Omega(p)/\Omega(0)$—, and the individual frequencies $\Omega_j(p)$

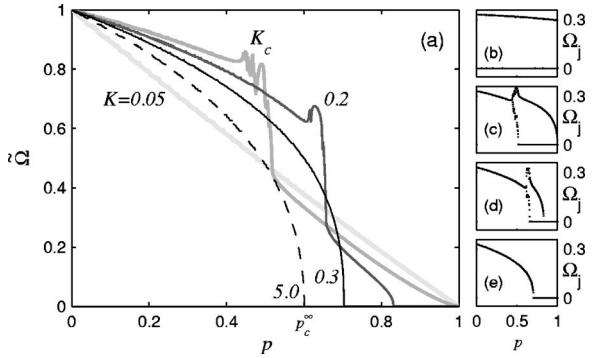

FIG. 3. (a) Normalized ensemble's frequency $\tilde{\Omega}(p)$ for different values of the coupling strength K in a population of oscillatory and excitable ML units ($N=500$). The dashed line for large coupling ($K=5$) shows the convergence of p_c to the value predicted by Eq. (6). Panels (b)–(e) show the individual frequencies for $K=0.05$ (PO) (top), $K_c\simeq 0.144$, $K=0.2$, and $K=0.3$ (transition GO-Q) (bottom).

(right panels) for different values of K. Note that for small coupling the transition to *quiescence* ($\tilde{\Omega}=0$) occurs trivially at $p_c=1$. Such behavior changes above $K_c\simeq 0.144$, where the transition begins to take place at $p_c<1$. Also, note that for intermediate values of K the curves present a steplike profile, corresponding to the stripe-shaped region in Fig. 2(a). This can be seen in Figs. 3(c) and 3(d) where, in the corresponding range of p, the two observed frequencies in the ensemble are not 1:1 (neither 1:0) related.

The quantity Ω presents interesting universal properties around K_c. Assuming that Eq. (4) exhibits a SN bifurcation at some $p_{sn}(K)$ we have $p_c=1<p_{sn}(K)$ (for $K<K_c$), $p_c=1=p_{sn}(K)$ (at $K=K_c$), and $p_c=p_{sn}(K)<1$ (for $K>K_c$). And noting that (i) only the active (self-oscillating) elements contribute to Ω: $\Omega=(1-p)\Omega_A$. $[\Omega_E=0]$, and that (ii) in a SNIC, the frequency of the oscillating elements scales as a square root: $\Omega_A\simeq h(p_{sn}-p)^{1/2}$, we find that Ω grows from zero as a power of the distance to the critical p_c:

$$\Omega = (1-p)h(p_{sn}-p)^{1/2} \propto (p_c-p)^\beta, \tag{8}$$

with three different values of the exponent β: 1 (for $K<K_c$, $p_{sn}>p_c=1$), $\frac{3}{2}$ (at $K=K_c$, $p_{sn}=p_c=1$), $\frac{1}{2}$ (for $K>K_c$, $p_{sn}=p_c<1$).

In a neighborhood of $(K=K_c,\ p=1)$, we may obtain a universal scaling function by assuming that the shift of p_{sn} is approximately linear on K: $p_{sn}\simeq 1+g(K_c-K)$. Recalling that $p_c=1$ for $K\leqslant K_c$, we obtain from Eq. (8) the expressions

$$\Omega = h(p_c-p)[p_c-p+g(K_c-K)]^{1/2}, \quad (K\leqslant K_c)$$

$$\Omega = h(1-p)(p_c-p)^{1/2}, \quad (K>K_c). \tag{9}$$

These distinct scalings may be condensed into the single scaling function [by approximating $1\simeq p_c-g(K_c-K)$ in the second equation]:

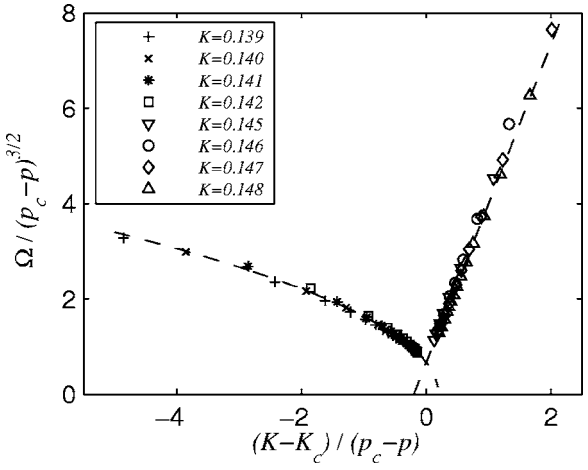

FIG. 4. Fitting to Eq. (10) for an ensemble of $N=1000$ ML elements, $K_c=0.14\,386(0)$. Dashed lines stem from Eq. (10) with fitting parameters $g=5.01$ and $h=0.66$.

$$\Omega = h(p_c - p)^{3/2}\Phi\left(g\frac{K-K_c}{p_c-p}\right), \tag{10}$$

with $\Phi(x)[=\sqrt{1-x}(x<0)]$, $[=1+x(x>0)]$. We obtain then two scaling regions with common fitting parameters g and h, see Fig. 4.

It is important to note that the scaling in Fig. 4 coincides with the one reported in [4] for the *amplitude* of oscillations in a mixed population of oscillators close to a Hopf bifurcation. Such coincidence lies in the same asymptotic dependence (square-root law) for the cycle's amplitude in the case of a Hopf bifurcation and for the cycle's frequency in the case of a SNIC.

In conclusion, we have demonstrated that for systems close to a SNIC, a transition to global quiescence occurs as the ratio p of excitable elements in the ensemble exceeds a certain value p_c. Such transition is a generalization of the aging transition reported in [4] and is characterized by a universal scaling function relating the mean frequency Ω with p and the coupling strength K. Additionally, we derive an analytical estimation for p_c in the large K limit which holds for both Hopf- and SNIC-mediated aging transitions.

Our results might be of importance in several situations, since excitability is a typical feature of many physical, chemical, and biological systems. Hence, our work is a first step in modeling the competition between excitable and oscillatory dynamics, with possible extensions to extended media and complex networks. Finally, our findings could also be relevant in populations of excitable systems when some of the elements turn self-oscillatory due to the presence of noise (coherence resonance [18]), a situation common in neuroscience.

Helpful comments from M. A. Matías are gratefully acknowledged. We also thank C. Monterola and G. Kalosakas for a critical reading of the manuscript.

[1] A. T. Winfree, *The Geometry of Biological Time*, 2nd ed. (Springer, New York, 2001).
[2] Y. Kuramoto, *Chemical Oscillations, Waves, and Turbulence* (*Springer-Verlag*, Berlin, 1984).
[3] A. S. Pikovsky, M. G. Rosenblum, and J. Kurths, *Synchronization, a Universal Concept in Nonlinear Sciences* (Cambridge University Press, Cambridge, 2001).
[4] H. Daido and K. Nakanishi, Phys. Rev. Lett. **93**, 104101 (2004).
[5] E. Meron, Phys. Rep. **218**, 1 (1992).
[6] J. P. Keener and J. Sneyd, *Mathematical Physiology* (Springer, New York, 1998).
[7] F. C. Hoppensteadt and E. M. Izhikevich, *Weakly Connected Neural Networks* (Spinger-Verlag, New York, 1998).
[8] M. R. Rosen, Heart Rhythm **2**, 418 (2005).
[9] J. Miake, E. Marbán, and H. Bradley Nuss, Nature (London) **419**, 132 (2002).
[10] Y. A. Kuznetsov, *Elements of Applied Bifurcation Theory* (Springer-Verlag, New York, 1998).
[11] J. Rinzel and B. Ermentrout, in *Methods in Neuronal Modelling: From Ions to Networks*, edited by C. Koch and I. Segev (MIT Press, Cambridge, 1989), pp. 251–291.
[12] S. K. Han, C. Kurrer, and Y. Kuramoto, Phys. Rev. Lett. **75**, 3190 (1995).
[13] C. Morris and H. Lecar, Biophys. J. **35**, 193 (1981).
[14] B. Ermentrout and N. Kopell, SIAM J. Appl. Math. **50**, 125 (1990).
[15] M. C. Eguia, G. B. Mindlin, and M. Giudici, Phys. Rev. E **58**, 2636 (1998).
[16] S. Shinomoto and Y. Kuramoto, Prog. Theor. Phys. **75**, 1105 (1986).
[17] Y. Maistrenko, O. Popovych, O. Burylko, and P. A. Tass, Phys. Rev. Lett. **93**, 084102 (2004).
[18] A. S. Pikovsky and J. Kurths, Phys. Rev. Lett. **78**, 775 (1997).
[19] $g_L=0.5$, $V_L=0.4$, $C=g_{\mathrm{Ca}}=V_{\mathrm{Ca}}=1$, $g_K=2$, $V_K=0.7$, $v_{1,2,3,4}=(-0.01,0.15,0.1,0.145)$, $\lambda_0=0.33$.
[20] It has been introduced to account in the simplest way for the pacemaker (dubbed "funny") current present in the cardiac pacemaker cells. This current is active for a small membrane potential and vanishes just after the action potential upstroke ($V\sim 0.2$).
[21] The point $K_1=0.8205,\ldots$, where the line limiting PO touches the axis $p=0$ can be approximated by an expansion in powers of $\beta\equiv b_E-1$: $K_1^2=4\beta/3+O(\beta^2)$. Taking $\theta_A=t$, from the nonautonomous ODE: $\dot{\theta}_E=1-b_E\sin\theta_E+K\sin(t-\theta_E)$, K_1 can be estimated thanks to the symmetries of the saddle-node solution.
[22] Equation (6) has been validated with a population of oscillators of the type proposed in [15].